



PORTFOLIO

Application to Ph. D. Program

Ye Seo Park

Ye Seo Park

yeseopark@pitt.edu



University of Pittsburgh

Master of Science in Chemical Engineering

Cumulative GPA: 3.667 / 4.00

Advisor: Prof. Kenneth L. Urish

Inha University

Master of Science in Chemical Engineering

Cumulative GPA: 4.00 / 4.00 (4.44 / 4.50)

Advisor: Prof. Sang Eun Shim

Inha University

Bachelor of Science in Chemical Engineering

Cumulative GPA: 3.39 / 4.00 (3.58 / 4.50)

Dankook University

Bachelor of Science in Animal Resources Sciences

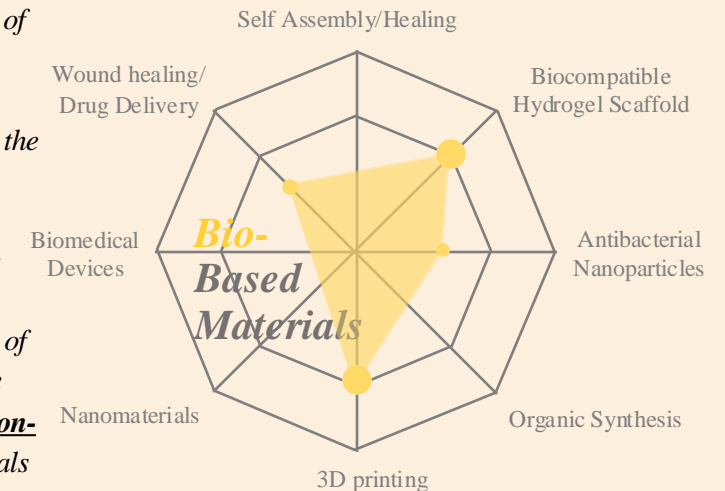
Cumulative GPA: 3.78 / 4.00 (4.08 / 4.50)

Publications

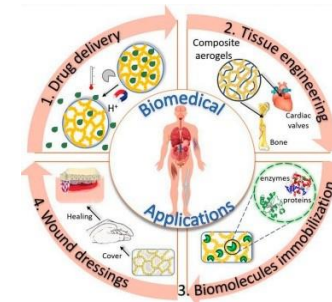
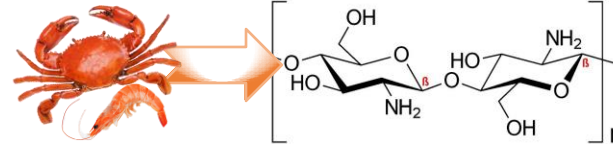
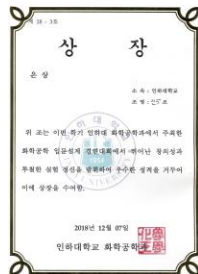
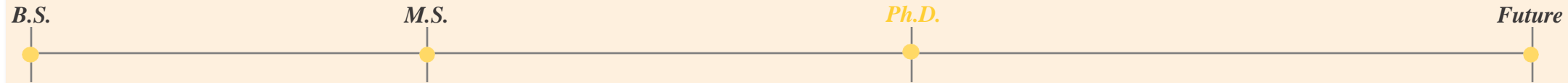
- 1) **Y. Park**, J.Choi, B. Kim, S.H. Baek*, S. E. Shim * and Y. Qian *, “Synergistic effects of P and Si on the flame retardancy in a polymethylsilsesquioxane aerogel prepared under ambient pressure drying”, 05.11.2023, <https://doi.org/10.1007/s10973-023-12244-8>.
- 2) *D. Shin, *S. Hwang, **Y. Park**, J. Kim, S. Lee, S. Hong, Y. Qian*, S. E. Shim *, “Rapid and Efficient Antibacterial Activity of Molybdenum-Tungsten Oxide from n-n Heterojunctions and Localized Surface Plasmon Resonance”, Applied Surface Science, 2022.09.01, <https://doi.org/10.1016/j.apsusc.2022.153496>.
- 3) B. Kim, J.Choi, **Y. Park**, Y. Qian, S. E. Shim *, “Semi-rigid polyurethane foam and polymethylsilsesquioxane aerogel composite for thermal insulation and sound absorption”, Macromolecular, 2022.04.30, <https://doi.org/10.1007/s13233-022-0026-8>.

“An aerogel, which I was interested most in research during my graduate studies, is the lightest solid material in the world and the first novel material I’ve touched since starting graduate studies. Learning silane aerogel synthesis and sol-gel chemistry, my curiosity got the better of me and I was able to fabricate the polymethylsilsesquioxane aerogels. altering the variables, differentiating the kinetics of hydrolytic condensation, and analyzing their properties, now I got a better understanding of the aerogel how it can be formed through the sol-gel process, and how the reaction rates of hydrolyzation and condensation. I could think of the idea of flame retardants being adapted to the aerogels from the burndown of our laboratory during the second semester and designed the experimental plan with environmentally friendly flame retardants. Despite a limited situation for experiments, I could learn the vacuum distillation unit and the organic synthesis to produce flame retardant-derivative silanes. Meanwhile, I could find a biodegradable material named chitosan, which also can act as a flame retardant with a synergistic effect of N and P elements for developing organic-inorganic hybrid aerogel under supercritical fluid drying conditions. Besides this, I’m investigating the structural tendencies of polymethylsilsesquioxane aerogel with different alcoholic solvents and contributing to the visualization of the article about the antibacterial activity of Molybdenum-Tungsten oxide. At the University of Pittsburgh, I also could reach the master’s degree with my research interest which is synthesizing antibacterial Au@Ag nanoparticles and simulating the S. aureus bacterial behavior with Joint-on-a-chip by optimizing the flow rate of medium and incubation time. For my Ph.D, I have a strong desire to broaden my knowledge of biomaterials like biocompatible hydrogel scaffolds for tissue engineering and antibacterial nanomaterials applied for biomedical devices.

☺ My Interests



Heading to the Dream



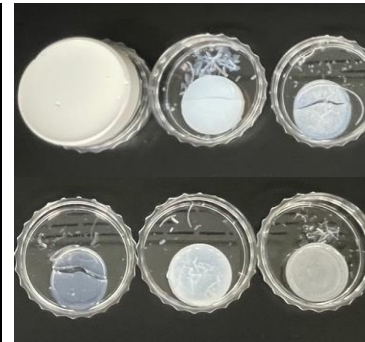
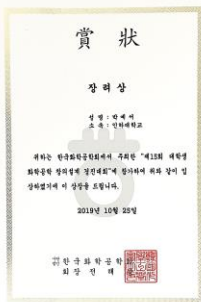
Applications of aerogels in the biomedical field
Loredana Nita et. al., Pharmaceutics 2020, 12, 449

Interests

- Conducting an undergraduate project on aerogels as well as such exposure and study of polymethylsilsesquioxane aerogels shaped **my vocation to fabricate diverse aerogels.**
- Expecting to learn about hydrogels with fascinating properties in biomedical fields.

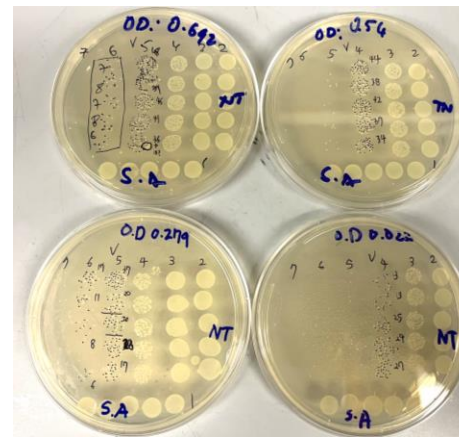
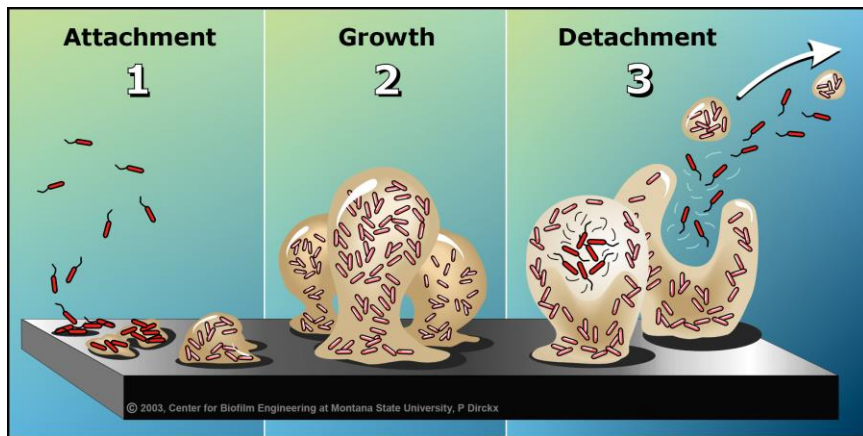
Researches

- Develop the fire retardant properties and thermal stability properties of polymethylsilsesquioxane aerogel by introducing the N-, P- containing materials.
- Design the polymethylsilsesquioxane aerogel with various degrees of transparency, mechanical strength and shrinkage degree with various alcoholic solvents.
- Passion about a better **understanding of controlling the nanomaterials and application of biomaterials.**



Characterizing Hydrogels for Use in Drug Delivery Systems
Vitl Life Science Solutions 2017, Jan 3

Adult Reconstructive and Arthroplasty Orthopedic Laboratory Lab

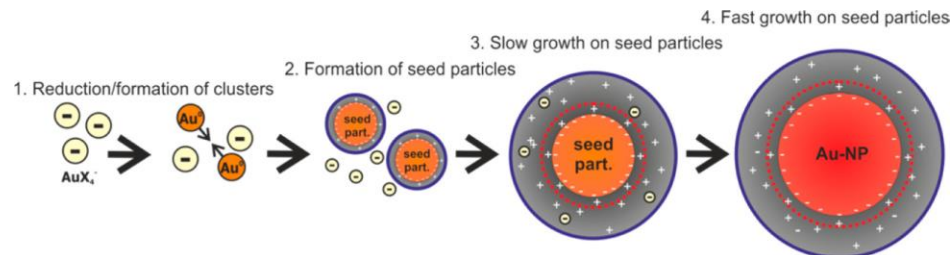


Skills

- UNIVERSITY OF PITTSBURGH (2022.09~Present)**
Master student in Chemical and Petroleum Engineering
Cumulative GPA: 3.429 / 4.00.
- Acquired the knowledge of chemical reaction, transport phenomena, thermodynamic using COMSOL, MATLAB and Python and learned data statistics and ODE calculation using Python in CheM core courses.
- Acquired the knowledge of COVID viruses and mechanisms of biofilm such as quorum sensing gene signaling from 'Advanced Microbiology' class in CMU.

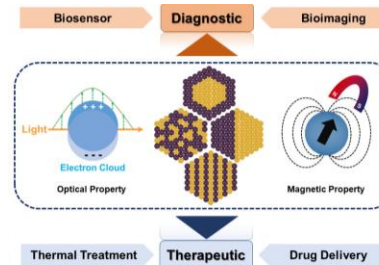
Researches

- Synthesized bimetallic Au@Ag nanoparticles.
- Analyzed nanoparticles with UV-Vis, DLS, SEM, TEM and EDX.
- Learned how to culture bacteria and analyzed *S. aureus* bacteria growth (CFU) and bacteria growth inhibition with different concentrations of antibacterial nanoparticles (MIC) using Microplate Reader OD600.
- Simulated *S. aureus* bacterial behavior in a multichamber bioreactor (Joint-on-a-chip) with different flow rates of medium or incubation times.



Turkevich in New Roles: Key Questions Answered for the Most Common Gold Nanoparticle Synthesis.
Wuithschick, M et. al, ACS Nano 2015, 9 (7), 7052-7071.

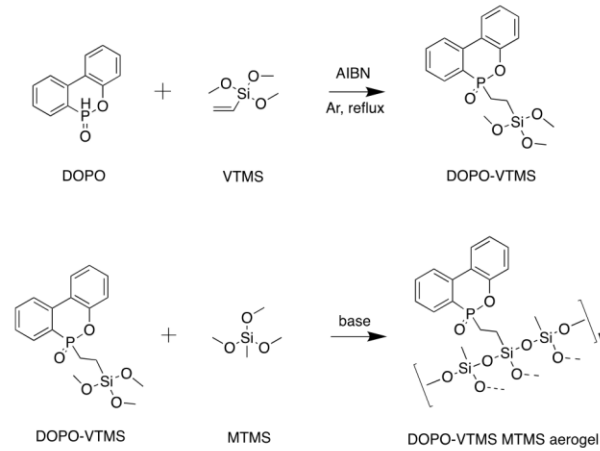
Bi metallic Nanoparticles: Enhanced Magnetic and Optical Properties for Emerging Biological Applications. Sinoi P et. al, Appl. Sci. 2018, 8(7), 1106





Academic Experiences

1. Synergistic effects of P and Si on the flame retardancy in a polymethylsilsesquioxane aerogel prepared under ambient pressure drying (Accepted)



Scheme 1. Schematic of DOPO-VTMS synthesis

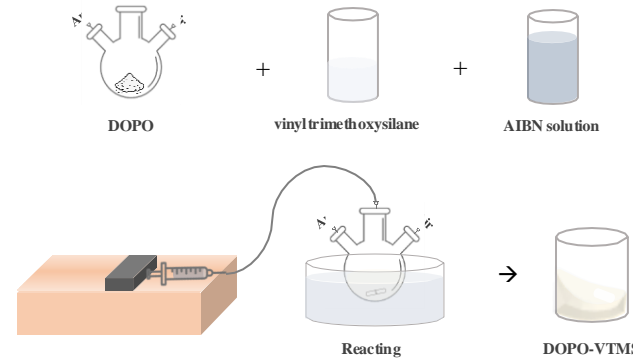


Figure 1. Synthesis of DOPO-VTMS

Recently, 9,10-dihydro-9-oxa-10-phosphaphenanthrene-10-oxide (DOPO) is used as **the most renowned environmentally friendly flame retardants**. Its own environmentally friendly property has the powerful strength and more promising comparable to other flame retardants since it does not release any halogen when it is burnt. For limited flame retardant properties of polymethylsilsesquioxane aerogel, this halogen-free DOPO is introduced in the aerogel in attempt to improving their flame retardancy, but pure DOPO in polymethylsilsesquioxane aerogel rather did have an adverse effect on the flame retardancy compared to original aerogel. Instead of introducing only DOPO, DOPO can be combined with vinyltrimethoxysilane (VTMS), one of trimethoxysilane precursors by breaking vinyl site with azobisisobutyronitrile (AIBN), which resulted in the viscous oil, and this DOPO-VTMS can be synthesized with polymethylsilsesquioxane aerogel. DOPO-VTMS can give a flame retardancy with synergistic effect of P and Si elements in combustion.

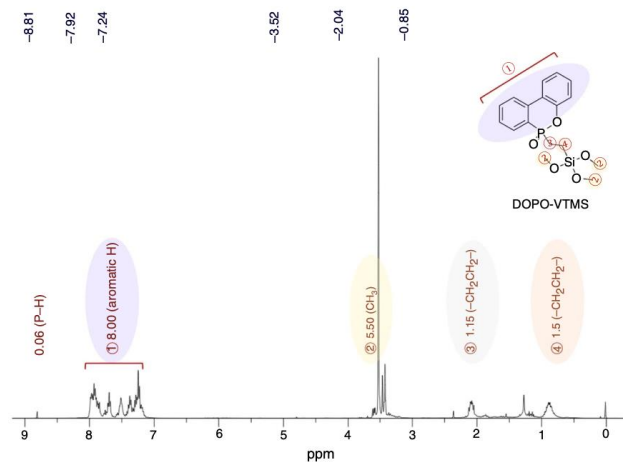


Figure 2. ^1H -NMR of DOPO-VTMS

In ^1H NMR, DOPO-VTMS had synthesized by linking DOPO and VTMS.

- By breaking vinyl group, C=C double bond (6 ppm) had disappeared thoroughly.
- The ratio of hydrogen bond in phosphorus group, phenyl group, and methoxy group is 0:8:9 and that of ethylene group is 1.5 as it can be seen in ① ~ ④.

- ① Aromatic H of DOPO
- ② RO-CH₃ of VTMS
- ③-④ -CH₂CH₂- of DOPO-VTMS

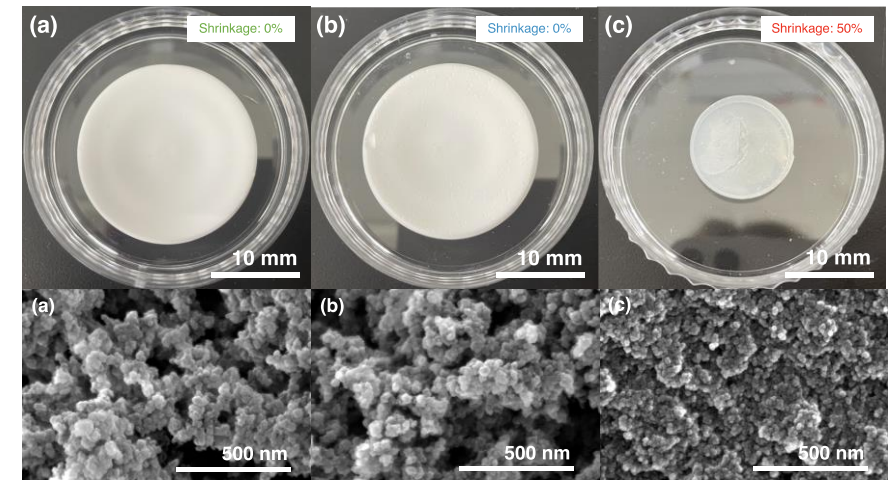


Figure 3. Digital images and SEM microphotographs of MTMS, DOPO MTMS and DOPO-VTMS MTMS aerogel

1. Synergistic effects of P and Si on the flame retardancy in a polymethylsilsesquioxane aerogel prepared under ambient pressure drying (Accepted)

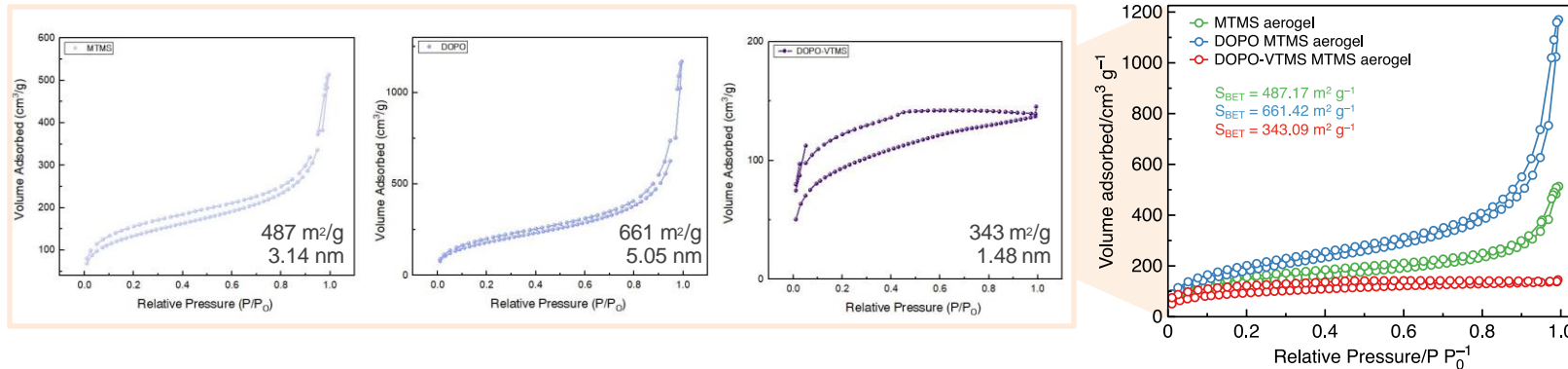


Figure 4. N₂ Isotherms of MTMS, DOPO MTMS and DOPO-VTMS MTMS aerogel

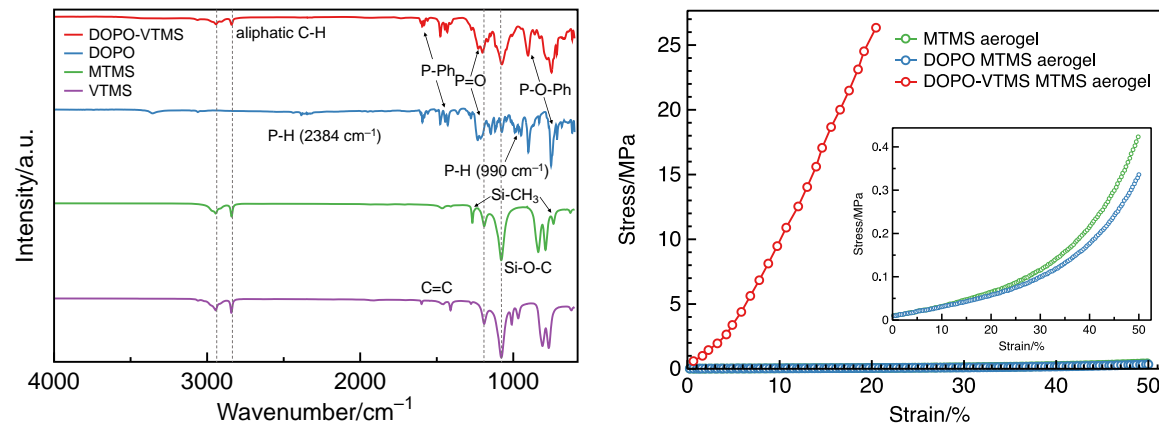


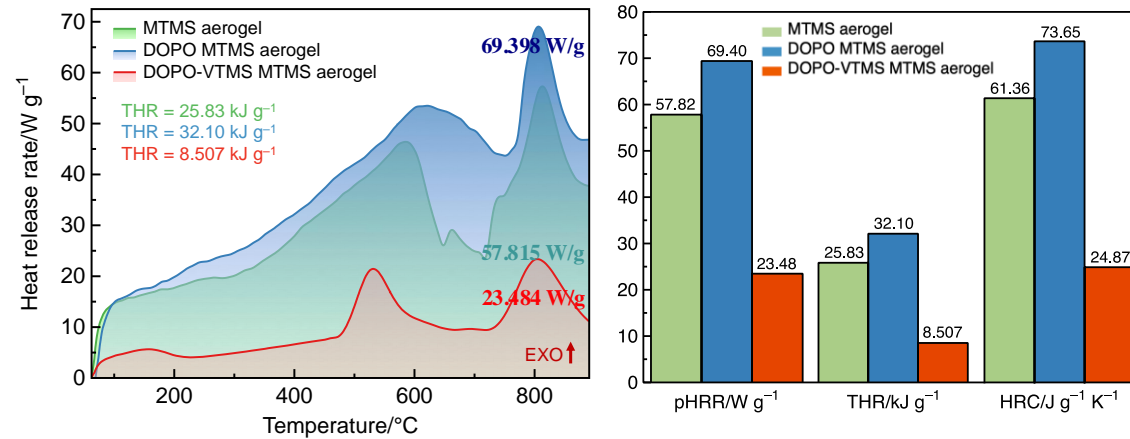
Figure 5. FT-IR graphs of each component and stress-strain compression curves of MTMS, DOPO MTMS and DOPO-VTMS MTMS aerogel

In N₂ Isotherms, two isotherm types of graphs are formed.

- MTMS and DOPO MTMS aerogels exhibit a Type II isotherm, classified by IUPAC, which corresponds to microporous and mesoporous structures.
- DOPO-VTMS MTMS aerogel exhibits a Type I isotherm, unimolecular microporous properties, having a relatively larger specific surface area than the other two aerogels despite shrinkage. A small amount of DOPO was taken off during the washing step, which might broaden the S_{BET} for the case with voids where DOPO was originally located in the DOPO MTMS aerogel.

- From the FT-IR spectra of MTMS, VTMS, and DOPO-VTMS, the peaks at 2944 and 2840 cm^{-1} can be attributed to C-H vibrations in aliphatic hydrocarbons, while the VTMS peaks at 1599 and 1410 cm^{-1} can be assigned to C = C vibrations. Double stretching vibrations between 800 and 900 cm^{-1} and peaks at 1078 and 1190 cm^{-1} are attributed to asymmetric Si-O-C vibrations in alkoxyasilanes. The peaks at 1267 and 780 cm^{-1} in the MTMS spectrum can be assigned to Si-CH₃ vibrations.
- The P-H stretching bands at 2384 cm^{-1} and the deformation vibration at 990 cm^{-1} in the DOPO spectrum disappear in the spectrum of DOPO-VTMS after the reaction of DOPO and VTMS, which correlates with the disappearance of the proton peak at 8.81 ppm from the ¹H-NMR spectrum (Fig. 2).
- In the spectra of DOPO and DOPO-VTMS, the P-Ph group is represented by bands at 1594 and 1477–1428 cm^{-1} and P = O vibration in the double bands around 1200 cm^{-1} . Bands at 901 and 750 cm^{-1} appear because of the asymmetric stretching vibration of the newly formed P-O-Ph bonds.
- The stress at fracture of the DOPO-VTMS MTMS aerogel is approximately 26.34 MPa, and 20% of the strain is attained in the compressive test without cracking, which is an unrivaled value compared to the other two aerogels. In contrast, the MTMS and DOPO MTMS aerogels exhibit much lower strengths of 0.42 and 0.34 MPa, respectively. The MTMS and DOPO MTMS aerogels show good flexibility with loading up to 50% strain but are fragile when compressed.
- The compression moduli of the MTMS, DOPO MTMS, and DOPO-VTMS MTMS aerogels are 0.007, 0.008, and 0.627 MPa; the compressive modulus of the DOPO-VTMS MTMS aerogel is 90 times higher than those of the MTMS and DOPO MTMS aerogels.

1. Synergistic effects of P and Si on the flame retardancy in a polymethylsilsesquioxane aerogel prepared under ambient pressure drying (Accepted)



67 % HRR Reduction

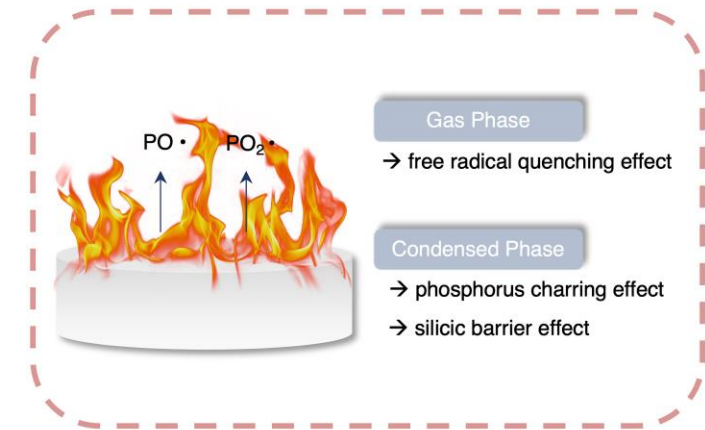


Figure 6. Microcalorimetry curves and pHRR, THR, and HRC values of MTMS, DOPO MTMS, and DOPO-VTMS MTMS aerogels Figure 7. Combustion mechanism of the DOPO-VTMS MTMS aerogel

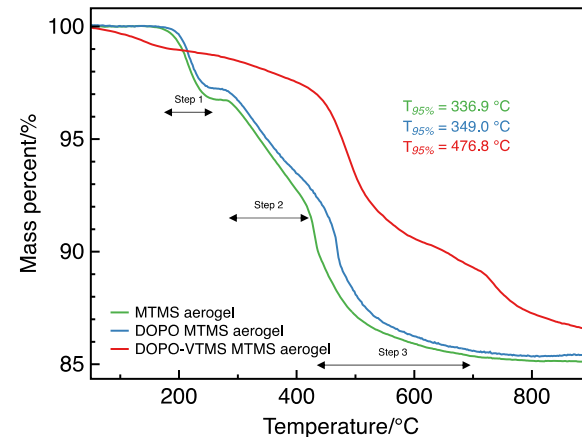


Figure 8. TG curves of MTMS, DOPO MTMS and DOPO-VTMS MTMS aerogel

From microcalorimetric analysis, DOPO-VTMS can act as a flame-retardant agent by reducing the pHRR value by 67% at 800 $^{\circ}\text{C}$.

- In MCC curves, MTMS aerogel has a pHRR value of 57.82 W g^{-1} in the second peak area whereas DOPO MTMS aerogel has the highest pHRR value of 69.40 W g^{-1} among the PMSQ aerogels, which implies that merely mixing DOPO and MTMS followed by the preparation of PMSQ aerogel has an adverse effect on flame retardancy of the PMSQ aerogel. Encouragingly, DOPO-VTMS MTMS aerogel exhibited the lowest pHRR value of 23.48 W g^{-1} .
- The first heat release peaks of the MTMS, DOPO MTMS, and DOPO-VTMS MTMS aerogels occur at 596, 600, and 530 $^{\circ}\text{C}$, respectively. The gradual slope can be matched to the TG curves, where the curve for the second decomposition step of the DOPO-VTMS MTMS aerogel exhibits a sharp decline, and the curves of the MTMS and DOPO MTMS aerogels decline gently. The second heat release peaks of the MTMS, DOPO MTMS, and DOPO-VTMS MTMS aerogels can be observed at approximately 800 $^{\circ}\text{C}$, which can be explained by the final decomposition, as seen in the TG curves.

In TG curves, the aerogels were heated from 100 $^{\circ}\text{C}$ to 900 $^{\circ}\text{C}$ with heating rate of 10 $^{\circ}\text{C}/\text{min}$.

- For MTMS and DOPO MTMS aerogels, the first degradation step (Step 1) is ascribed to the evaporation of water and solvents (180–250 $^{\circ}\text{C}$); Si-CH_3 then decomposes in the range of 250–420 $^{\circ}\text{C}$ (Step 2); and finally, methyl groups cause decomposition up to 700 $^{\circ}\text{C}$ (Step 3).
- DOPO affects the thermal stability of the MTMS aerogel by delaying decomposition; therefore, the peaks of the DOPO MTMS aerogels shift to the right.
- In contrast, DOPO-VTMS exhibits a sluggish decline of 3% mass loss up to 430 $^{\circ}\text{C}$, followed by a sharp decline above 430 $^{\circ}\text{C}$, which corresponds to the thermal behavior of DOPO-VTMS. Given this behavior, it can be assumed that introducing DOPO-VTMS into the PMSQ aerogel would retard the decomposition of Si-CH_3 and methyl groups through the formation of char during the three degradation steps.

1. Synergistic effects of P and Si on the flame retardancy in a polymethylsilsesquioxane aerogel prepared under ambient pressure drying (Accepted)

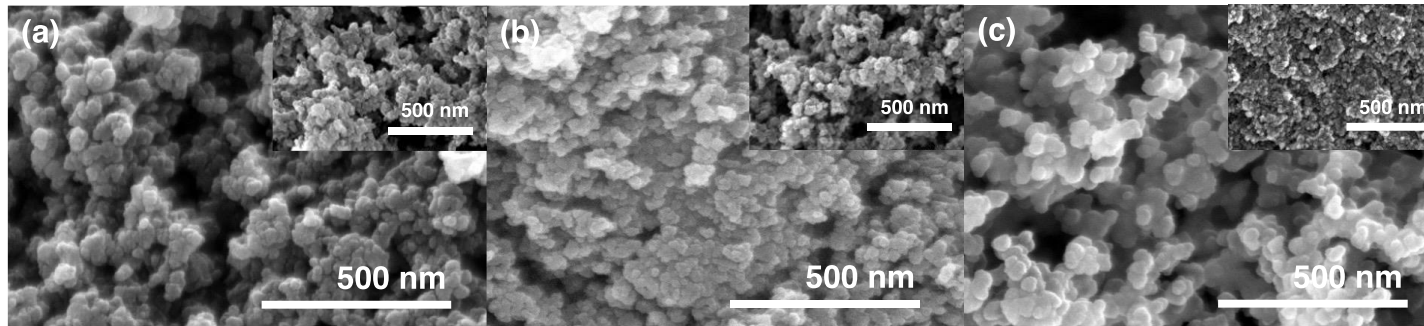


Figure 9. SEM images of the char residues of (a) MTMS, (b) DOPO MTMS, and (c) DOPO-VTMS MTMS aerogels

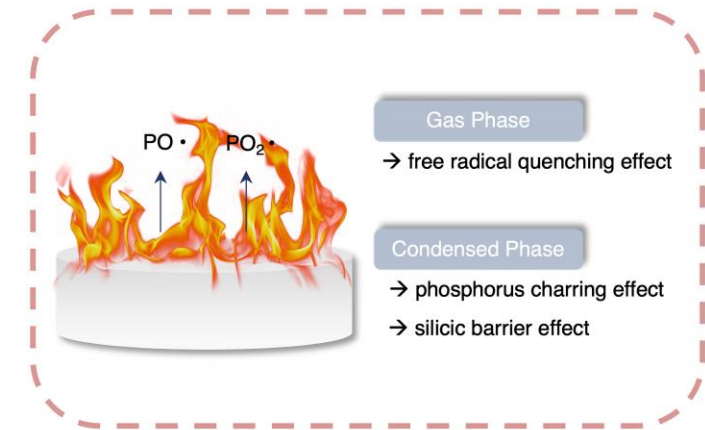
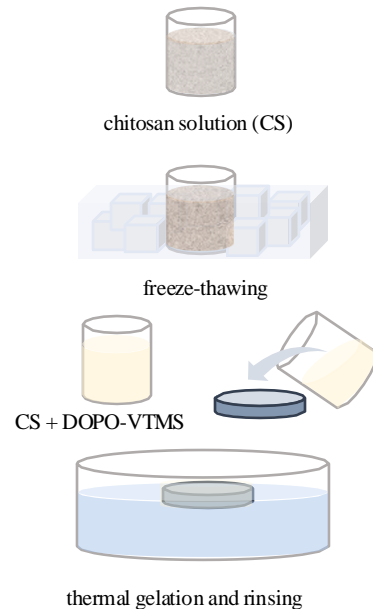


Figure 7. Combustion mechanism of the DOPO-VTMS MTMS aerogel

- DOPO-VTMS helps increase char formation and thickens the char layer more than DOPO does due to the synergistic flame-retardant effect of P and Si, attributing to the formation of P honeycomb barriers and additional Si physical barriers. The combustion behavior can be analyzed based on the synergistic effects of P and Si in the gas and condensed phases. In the gas phase, P suppresses combustion via the quenching effect of free radicals. The DOPO-VTMS structure captures hydrogen radicals, which prevents the further oxidation of volatilized products and inhibits flame propagation. Meanwhile, P has a charring effect since char formation is effectively promoted in the condensed phase. DOPO-VTMS can also form a synergistic char structure of P and Si, while MTMS and DOPO can only form a silica barrier or aromatic char. The char layers containing P and Si successfully prevent the decomposition of the MTMS aerogel. The formation of the $P(=O)-O-Si$ linkage of DOPO-VTMS simultaneously imparts synergistic flame retardancy in the gas and condensed phases. This can increase char formation in the condensed phase because interactions between the DOPO and VTMS can induce better flame retardancy than when only using Si or P alone. The interactions in the condensed phase play an important role in reinforcing the carbon layers with a robust phenyl and inorganic structure.
- Devolatilization is a decomposition process that occurs when volatile compounds are driven out from a hydrocarbon material being heated. It was found that there was no notable char remaining for the MTMS and DOPO MTMS aerogels, whereas the char layers for the DOPO MTMS aerogel were intumescent and firm. The MTMS aerogel may produce SiO_2 in the gas phase and carbonaceous products in the char layer; however, when PMSQ chemically bonded with DOPO could only interact in the condensed phase. As shown in the SEM images of the burned aerogels, there are different char morphologies in the PMSQ aerogels. The char becomes less porous and agglomerated in the MTMS and DOPO MTMS aerogels. However, the char morphology of the DOPO-VTMS MTMS aerogel becomes an open system after combustion because of the chemical combination of DOPO and VTMS, leading to the formation of a multi-porous char structure. The strength of the char increases, and a thicker char is formed, which is caused by the gaseous products during combustion and the volatilization of these gases.

2. A novel flame retardant DOPO-derivatives in a chitosan aerogel monolith: a synergistic effect of containing nitrogen, phosphorus and silicon



Freeze-thawing process of chitosan
Mixing of DOPO-VTMS and chitosan
Thermal gelation at 60 °C
Supercritical Drying

Scheme 1. Process of chitosan/DOPO-VTMS aerogel

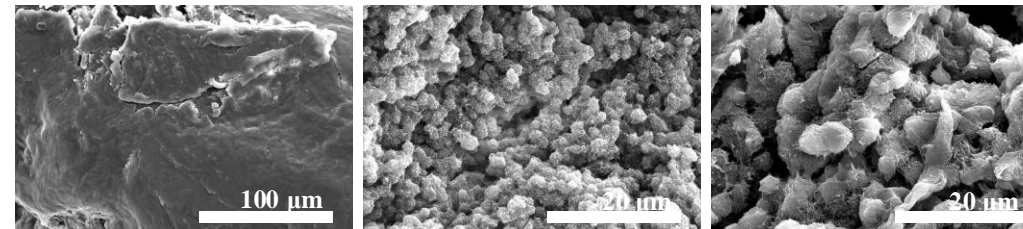
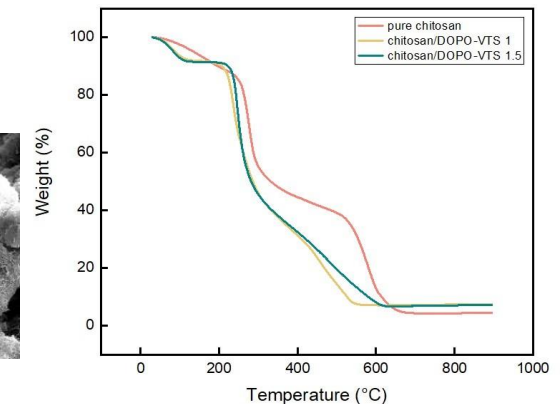


Figure 1. SEM microphotographs and TGA graphs of pure chitosan, chitosan/DOPO-VTMS 1 and chitosan/DOPO-VTMS 1.5 aerogel



- For the solvation of chitosan aerogel in base solution, freeze-thawing method was carried out. The concept of freezing is reducing the total energy of molecules and preventing the high molecular polymers mingled. When chitosan was dispersed uniformly in solution, DOPO-VTMS was introduced into chitosan solution and it started to gelate DOPO-VTMS thermally. After gelation, the solvent exchanging and supercritical drying were completed and the organic-inorganic hybrid aerogel can be made with various ration.
- In SEM microphotographs, pure chitosan aerogel had no porous structure so it can't be said to be aerogel which is composed of air almost with myriads of nano-sized pores. However, in chitosan/DOPO-VTMS aerogels, there are composed of the mingled nanoparticles with high porosity.
- In TGA graphs, there are somewhat difference of pure chitosan and chitosan/DOPO-VTMS aerogels with different decomposition temperatures. chitosan/DOPO-VTMS have higher $T_{95\%}$ than pure chitosan aerogel.
- When pure chitosan aerogel and chitosan/DOPO-VTMS aerogel are burnt, there was different tendencies in combustion. Both formed the charring, but pure chitosan aerogel altered the charred aerogel while the other disappeared like capturing the fire. As it can be seen at SEM microphotographs, there was a clear difference between them. It seemed they had different mechanisms, which chitosan/DOPO-VTMS has synergistic effect of N, P and Si elements for flame retardancy.

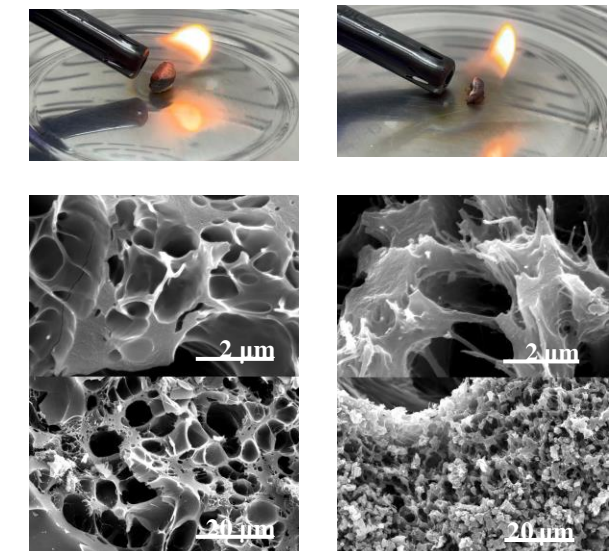


Figure 2. SEM microphotographs of char residues from pure chitosan and chitosan/DOPO-VTMS 1 aerogel

3. Investigation on the structures of polymethylsilsesquioxane aerogel with various alcoholic solvents

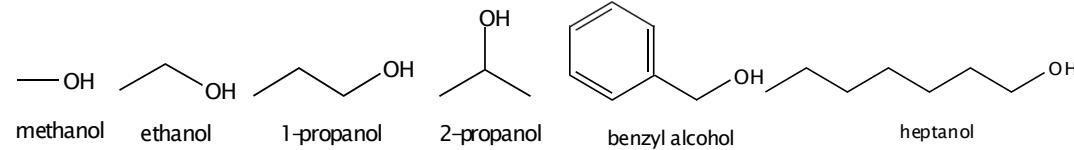
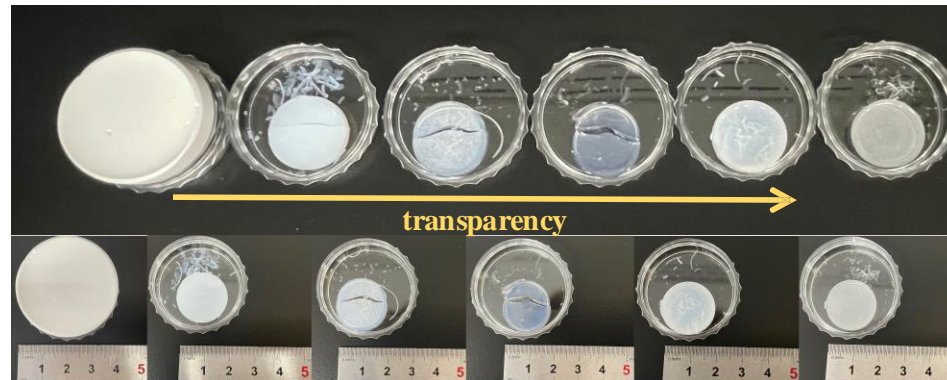


Figure 1. Chemical structures of various alcoholic solvents and images of polymethylsilsesquioxane aerogel



The purpose of this study is to investigate the tendency of the structures of polymethylsilsesquioxane aerogels by varying the alcoholic solvents (methanol, ethanol, 1-propanol, 2-propanol, benzyl alcohol and heptanol) used as the main variables to know the consistency of pore sizes or physical properties of silica aerogels. The longer chains of -OH group in the solvents it has, the more transparent it is. As the surface area increases and the pore size decreases, the polymethylsilsesquioxane aerogels show the inclination of transparency, which can be explained by the transmittance of the light and this transmittance can be proportional to the number of carbon by this experiment. Also, it contributes to the mechanical strength with having more carbon chains.

In N_2 Isotherms, several isotherm types of graphs are shown varying the solvents.

- Aerogel with methanol showed the uniform sizes of nanoporous and mesoporous with largest pore sizes, but when the -OH chains of the solvents is longer, pore sizes and surface areas got smaller due to the shrinkage. Likewise, aerogel with benzyl alcohol has a weak substrate with a mesoporous sizes.
- Aerogel with 2-propanol and heptyl alcohol have occurred capillary condensation and pore blocking. They had the smallest nano-sized pores among them, but their pores are mostly ink-bottle pores with different necks.

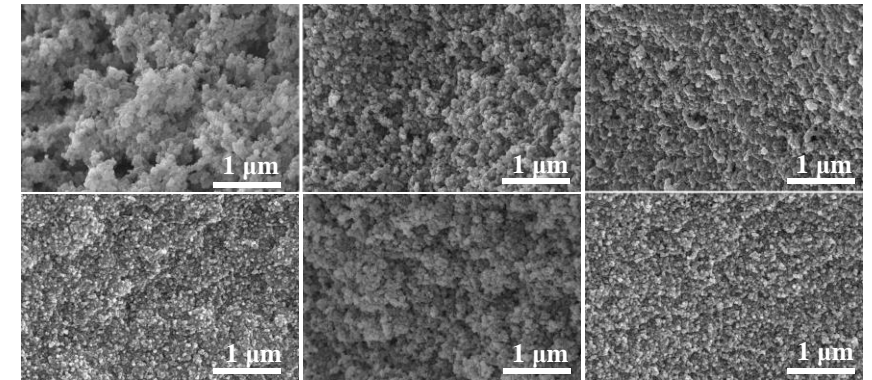


Figure 2. SEM microphotographs of aerogels with various alcoholic solvents

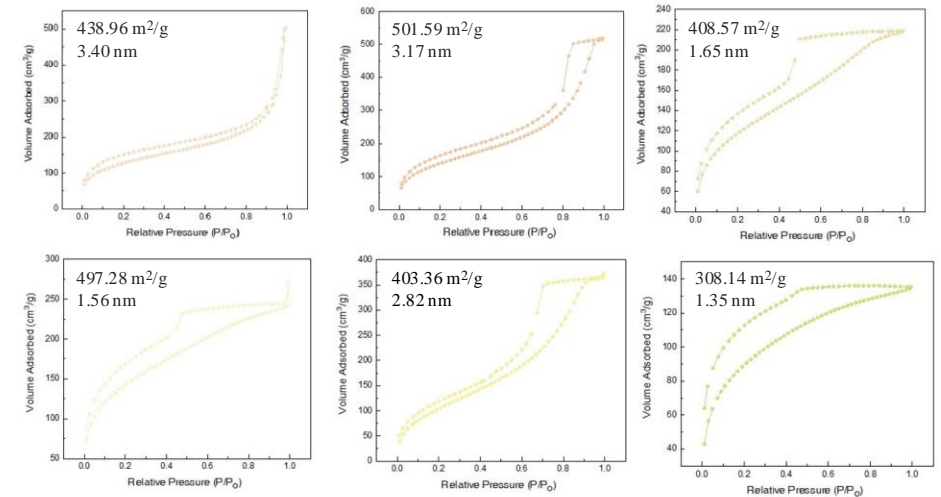
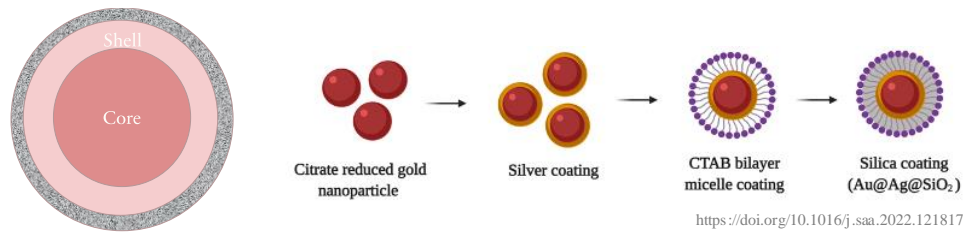


Figure 3. N_2 Isotherms of aerogels with various alcoholic solvents

4. Synthesis of bimetallic Au@Ag nanoparticles for antibacterial properties



Scheme 1. Design of surface-coated Au@Ag nanoparticles

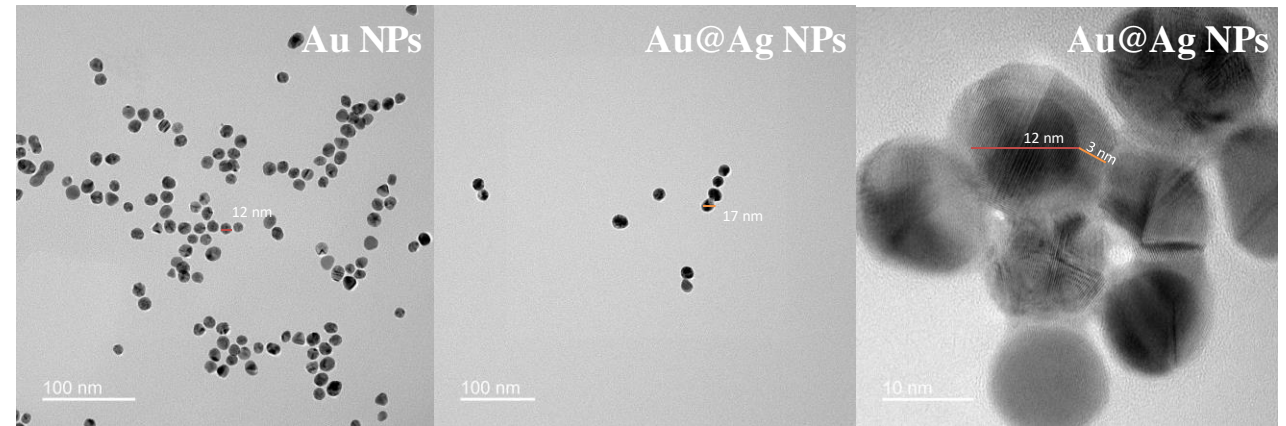


Figure 2. TEM microphotographs of Au and Au@Ag NPs solution

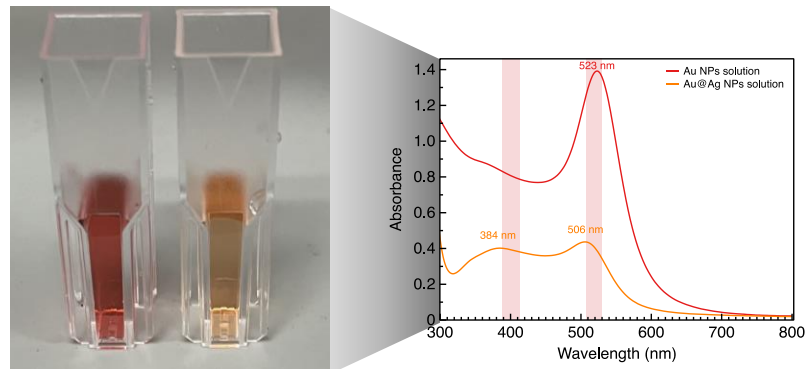


Figure 1. Images of Au and Au@Ag NPs solution (left) and UV-Vis spectrophotometer of Au and Au@Ag NPs solution (right)

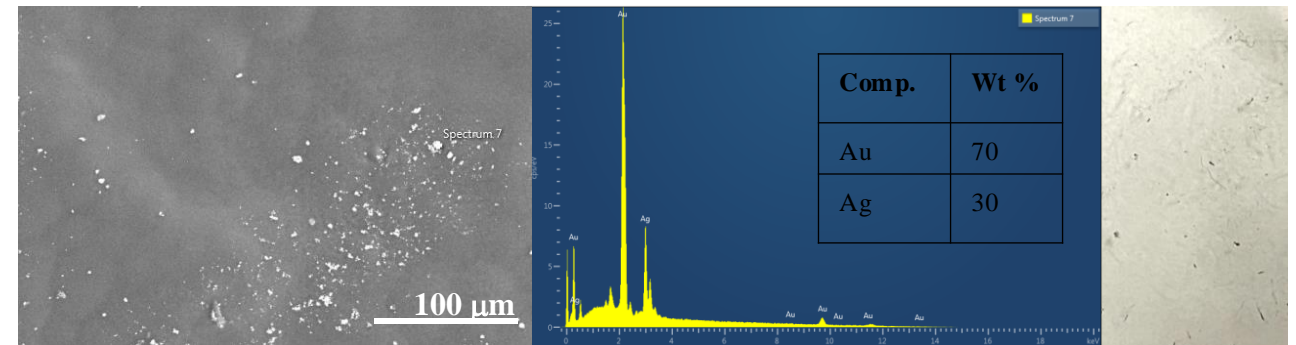


Figure 3. SEM microphotographs, EDX and images of Au@Ag NPs

4. Synthesis of bimetallic Au@Ag nanoparticles for antibacterial properties

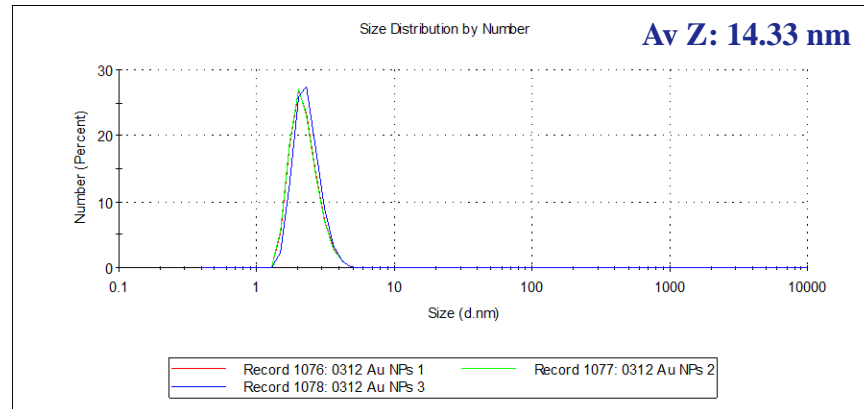


Figure 4. Dynamic Light Scattering of Au nanoparticles

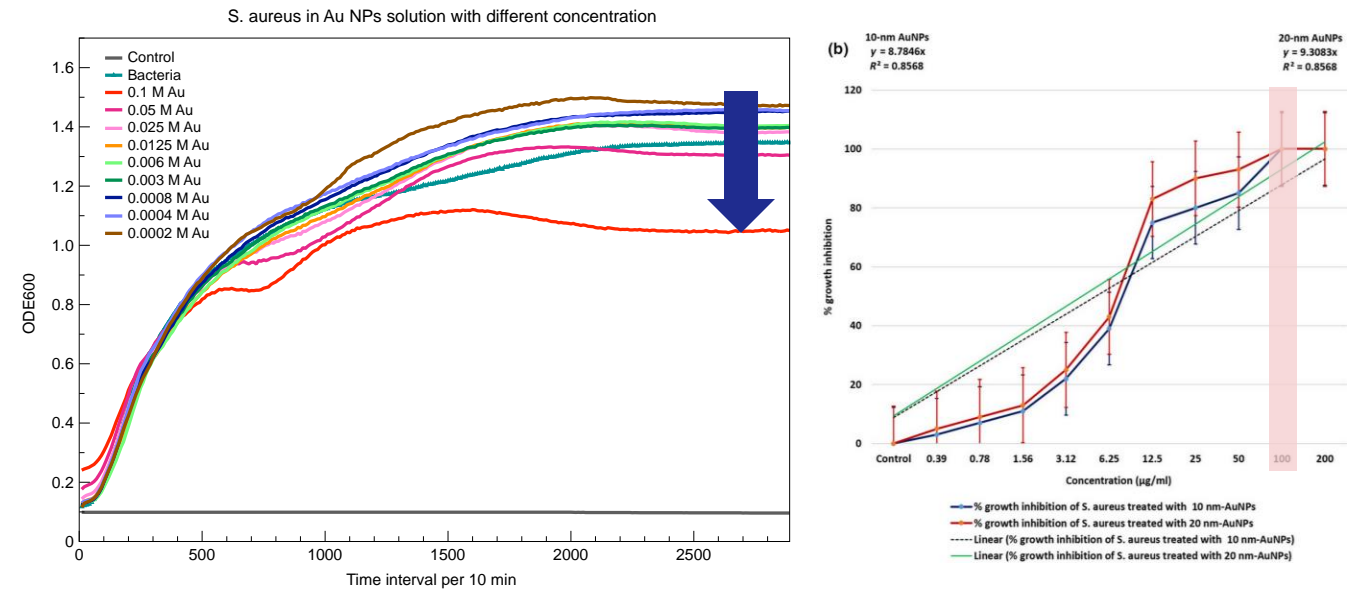
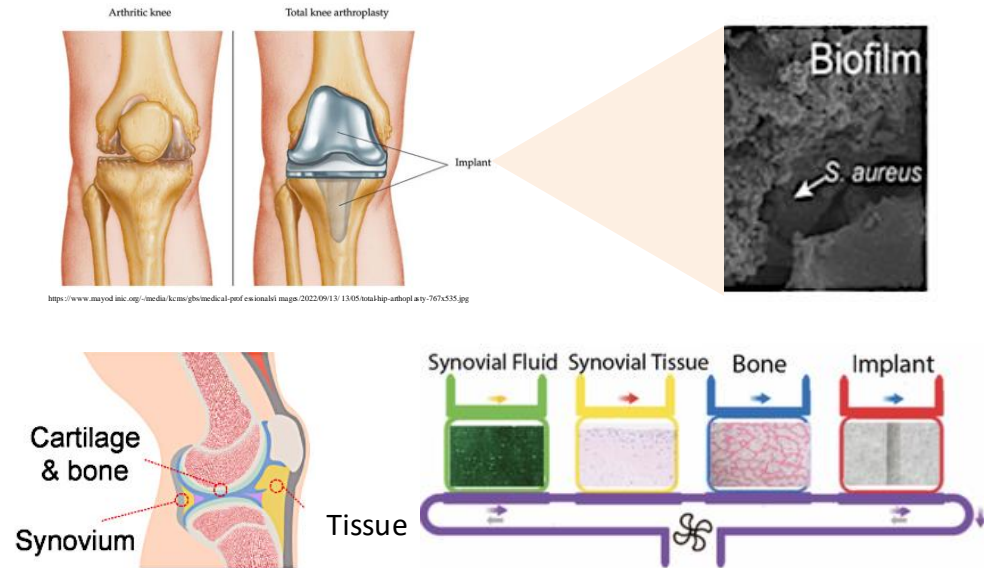


Figure 5. Exposure *S. aureus* to Au solution for antibacterial properties in 48 h growth curve.

Au@Ag NPs can be fabricated by Turkevich method where the crystal formation occurs by combining gold atoms or ions each other and growth as a particles with increasing the size of the original crystal structures by nucleation and the reduction of silver ions and deposition of silver atoms onto the gold nanoparticle surface results in the formation of bimetallic nanoparticles with a gold core and a silver shell. Gold nanoparticles are typically prepared by the reduction of gold ions using a reducing agent, sodium citrate, in an aqueous solution. The reduction process results in the formation of gold nanoparticles with a range of sizes and shapes, depending on the reaction conditions. Surface modification of Au@Ag nanoparticles (Silica-coated/Mesoporous structures) could be considered for multifunctional properties.

- In UV-vis spectrophotometer, 430 nm and 520 nm wavelength indicates silver and gold nanoparticles which corresponds to the orange and red color of nanoparticle solution .
- In DLS, size distribution exhibits monodispersity of size with Au nanoparticle diameter of 14.33 nm in average which was similar to the size measurement of TEM microphotographs.
- Exposure *S. aureus* to Au nanoparticle solution for antibacterial properties in 48 h growth curve depending on the different concentration of Au nanoparticle solution (0.0002 ~0.1 M)
- Compared to the reference, only 30 % of *S. aureus* growth was inhibited with 0.1 M Au nanoparticle solution, assuming that there were different conditions such as materials, synthesis and growth methods.

5. Investigation on *S. aureus* bacterial behaviors in a multichamber bioreactor (3D MiniJoint)



Human Mesenchymal Stem Cell-Derived Miniature Joint System for Disease Modeling and Drug Testing, Z. Li et. al, Adv. Sci. 2022, 9, 2105909

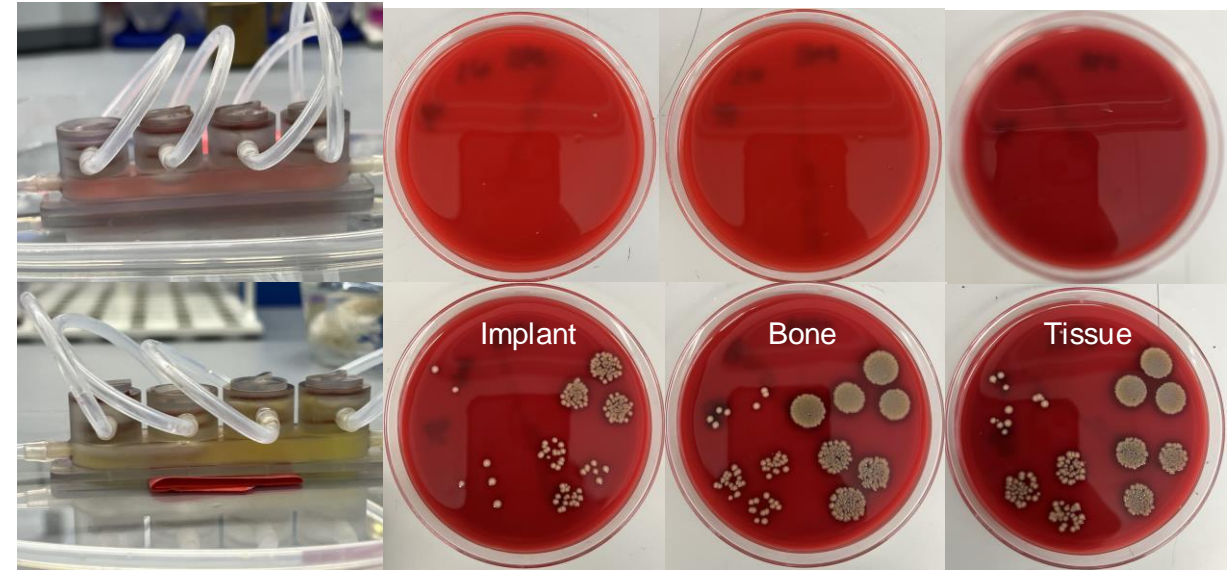


Figure 1. Biofilm assay for reference and *S. aureus* infection in each chamber (implant, bone, and tissue)

- The most common major surgical procedure in the United States is total knee arthroplasty (TKA). Periprosthetic joint infection (PJI; infected knee replacements) is the most severe complication in TKA and the largest cause of TKA revision (25%). Of great concern, the 5-year mortality after PJI is 20%, which is higher than most cancers. Bacteriophage therapy is a promising new approach for treating chronic PJI. The process involves obtaining preoperative bacteria cultures, screening a large phage library or cocktail of phages, and selecting a phage therapeutic with activity to the clinical isolate (bacteria culture). Matching a phage to a clinical isolate from the patient is necessary as phages bind specific surface receptors that can have large variations in the same species. In *Staphylococcus aureus*, the most common organism in PJI, phages primarily bind to wall teichoic acid (WTA), a peptidoglycan receptor. WTA can have a large phenotypic variation based on specific glycosylation patterns dependent on the local environments and growth states. Despite early success in this PJI case series, there remain some unexplained failures. A large gap in knowledge exists regarding the mechanism behind changes in phage activity between identical populations of bacteria and how changes in WTA glycosylation alter phage activity. The objective of this proposal is to determine how changes in *S. aureus* WTA glycosylation vary under different conditions and impact phage activity.
- In this work, we utilize the proven bioreactor design to form a PJI microJoint, with a 4-chamber configuration, maintained by a closed-loop tissue specific maintenance medium where chambers are interconnected by a separate common flow. Compartments will house one of 4 samples: pseudo-synovial fluid (PSF) with bacterial inoculate, synovial tissue, bone explant, and the implant embedded in an acellular hydrogel. In preliminary experiment utilizing a 4-chamber device (synovial fluid, synovial tissue, bone, and a titanium implant) 1×10^6 CFU *S. aureus* was used to inoculate the synovial fluid compartment. Planktonic bacteria was seen to proliferate and populate tissues in each compartment, forming an identifiable biofilm. This demonstrates that we can simulate biofilm formation in different micro-environments and therapeutic reduction by phage.

6. Photocatalytic crystalline titania/carbon-nanotube aerogels for antibacterial properties

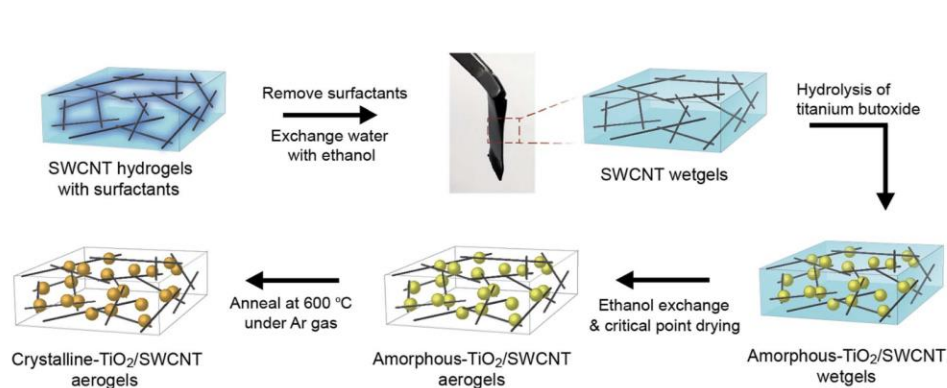


Figure 1. Photocatalytic TiO_2 /SWCNT Aerogel Synthesis

RSC Adv., 2016, 6, 22285

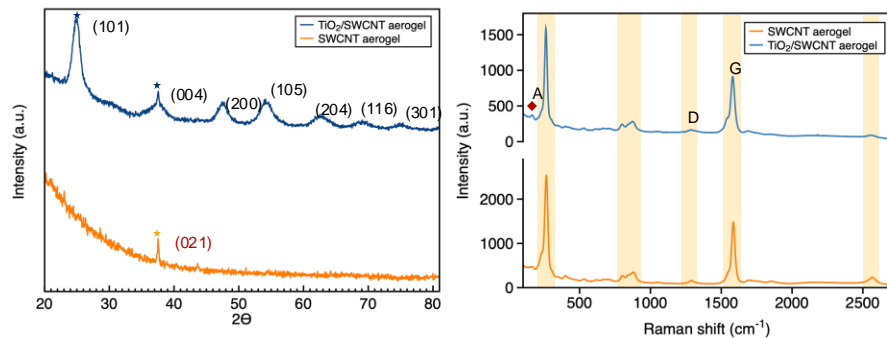
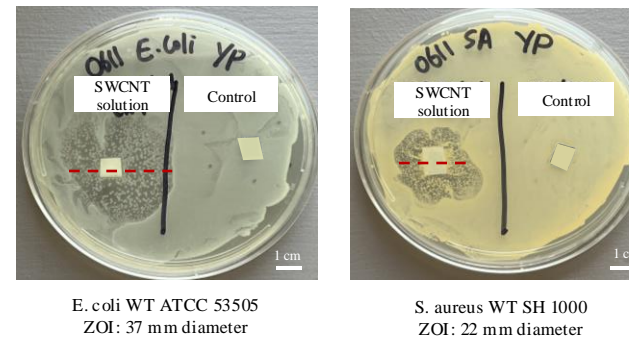


Figure 3. XRD patterns and Raman spectra of SWCNT and TiO_2 /SWCNT aerogels



E. coli WT ATCC 53505
ZOI: 37 mm diameter

S. aureus WT SH 1000
ZOI: 22 mm diameter

Figure 4. Disk diffusion test with 3 mg/ml SWCNT solution

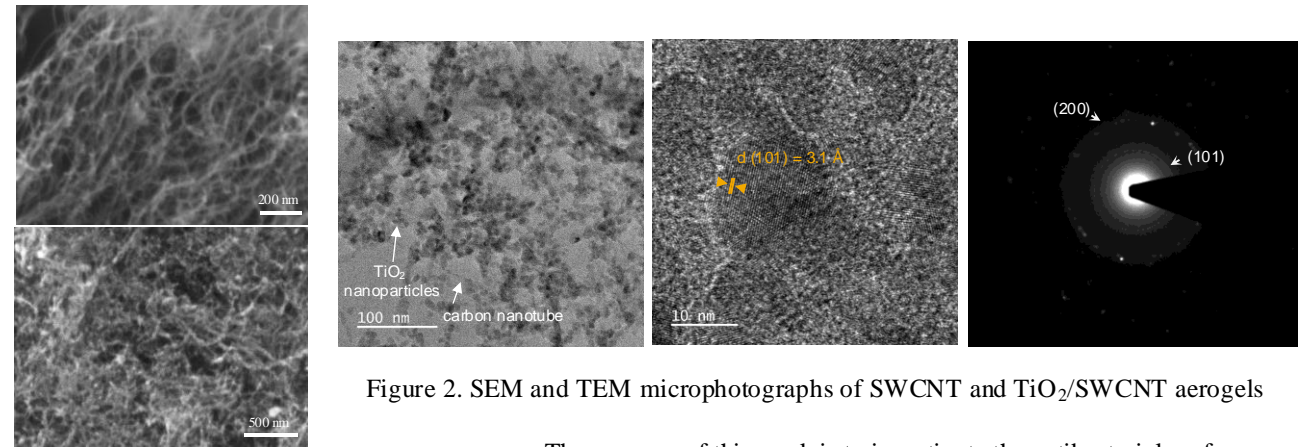


Figure 2. SEM and TEM microphotographs of SWCNT and TiO_2 /SWCNT aerogels

The purpose of this work is to investigate the antibacterial performances of photocatalytic titania/carbon nanotube aerogels under visible light irradiation. From reproducing the crystalline titania/carbon nanotube (TiO_2 /SWCNT) aerogel monolith to analyzing their crystallinity and chemical bonds from XRD and Raman spectroscopy, we aim to have improved antibacterial properties of TiO_2 /SWCNT aerogels under the visible light by performing different methods such as disk diffusion assay, agar dilution test, observation fluorescence by using mutant bacterial strains which adopted green fluorescent proteins to optimize the antibacterial assay. TiO_2 /SWCNT aerogels can be utilized for bacteria inactivation during water purification, wound dressing, or incorporation with textiles with the advantage of the use of natural sunlight.

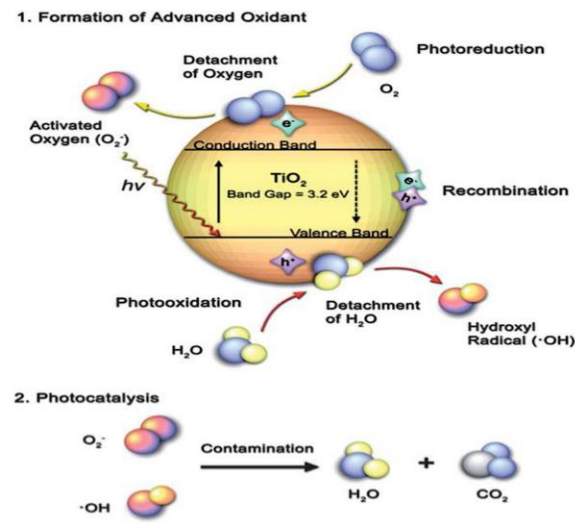
In XRD pattern of SWCNT and TiO_2 /SWCNT aerogels identifies the anatase phases of TiO_2 nanoparticles

- The different peaks of TiO_2 /SWCNT aerogels exhibit the anatase phases of TiO_2 nanoparticles, which accords the expected crystalline phase from the annealing temperature at 600 °C where titania crystallized to the anatase phase. The (101) and (004) peaks in the TiO_2 /SWCNT aerogel are prominently observed, indicating that the distinct anatase phase is well synthesized in crystalline TiO_2 /SWCNT aerogel.

Raman spectra of SWCNT and TiO_2 /SWCNT aerogels show the interactions between titania and SWCNTs

- Both SWCNT and TiO_2 /SWCNT aerogels have the same carbon peaks of D and G bands, characterizing the sp^3 -hybridized carbon at 1300 cm^{-1} and the sp^2 -hybridized carbon bonds at 1591 cm^{-1} and displayed radial breathing modes, which are exclusive features of SWCNTs, ranging in from 200 to 300 cm^{-1} . The Raman peak for anatase shows around 150 cm^{-1} .
- The ratio of I_D and I_G for TiO_2 /SWCNT aerogels decreased only to 0.18 from 0.11 for SWCNT aerogels, indicating only minimal damage to SWCNTs from titania deposition.

6. Photocatalytic crystalline titania/carbon-nanotube aerogels for antibacterial properties



Coatings 2019, 9(10), 613

Figure 5. Photoinactivation of bacteria with photocatalyst TiO_2

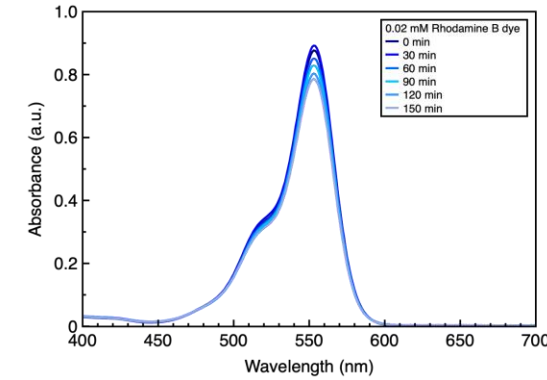


Figure 6. UV-vis spectra of photocatalytic Rhodamine B dye degradation with dye and $\text{TiO}_2/\text{SWCNT}$ aerogel

The photoinactivation of bacteria from $\text{TiO}_2/\text{SWCNT}$ aerogel under visible light irradiation through the photocatalytic mechanisms can induce improved reactive oxygen species (ROS) generation, oxidative stress, and direct killing against two Gram-positive *S. aureus* and Gram-negative *E. coli*. The photocatalytic performance was evaluated by observing the dye photodegradation rate under visible light irradiation with Rhodamine B dye solution as a control and $\text{TiO}_2/\text{SWCNT}$ aerogel. Their absorbance with each reaction time was observed and the degradation rate constant, k , was calculated using a pseudo-first kinetic order model.

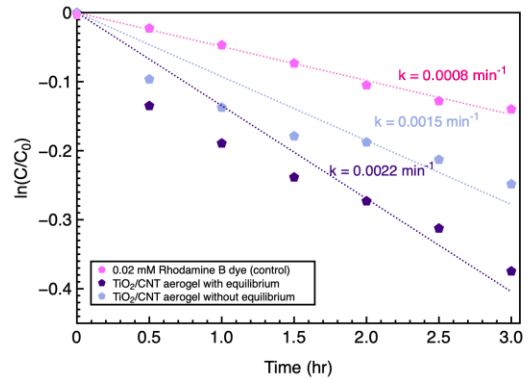
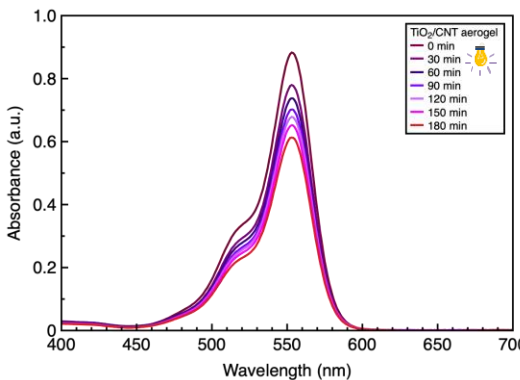


Figure 7. Photocatalytic Rhodamine B dye degradation kinetics for control and $\text{TiO}_2/\text{SWCNT}$ aerogels

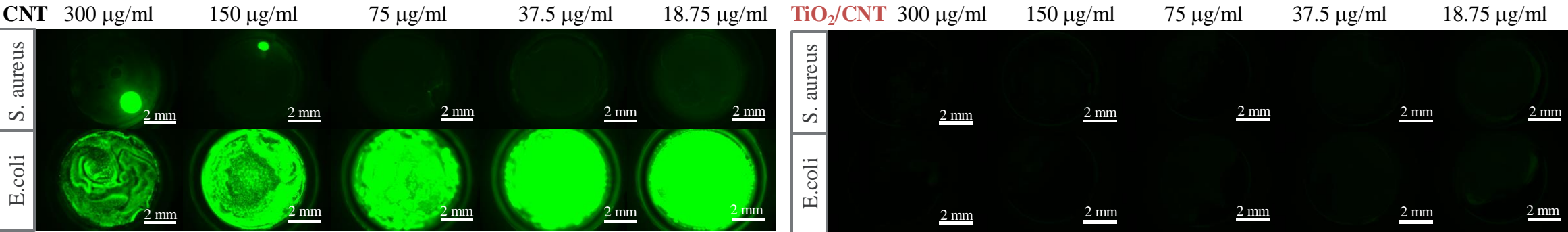
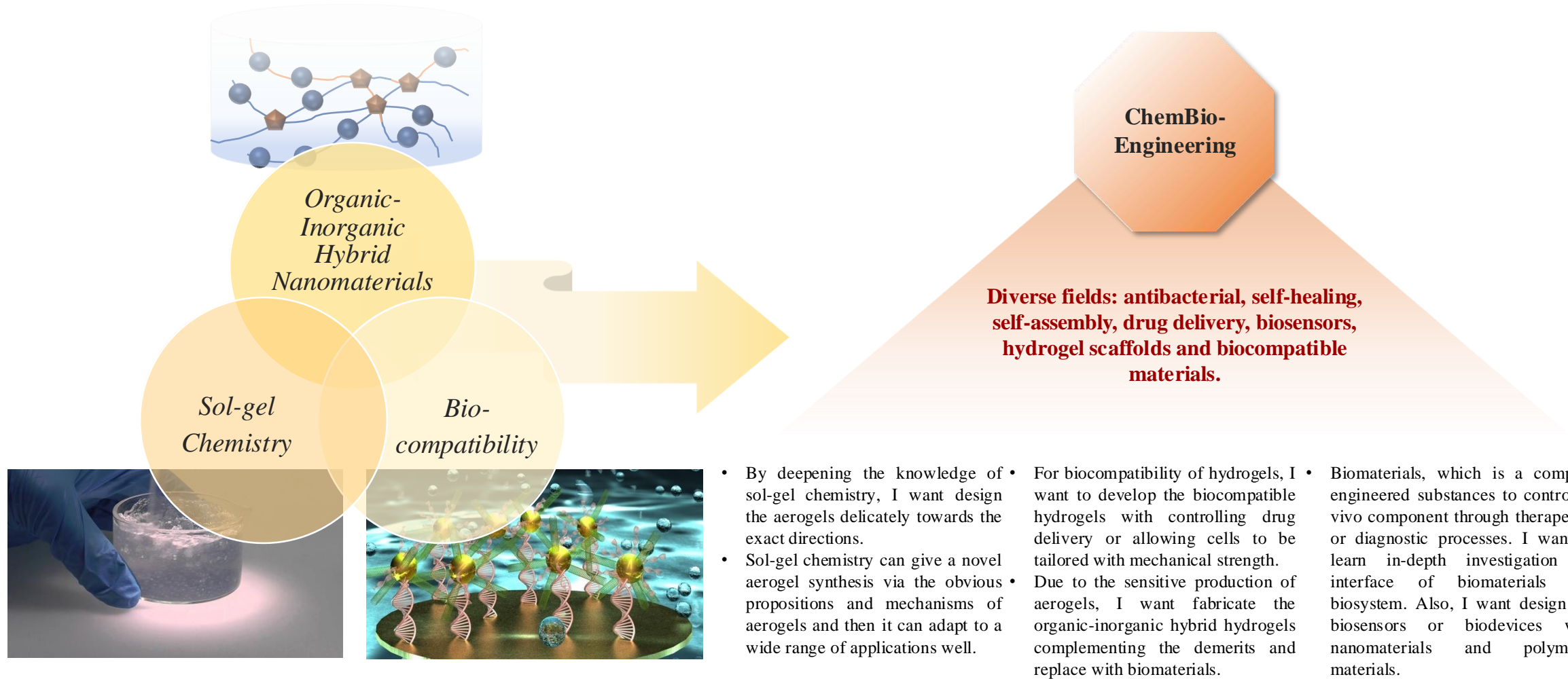
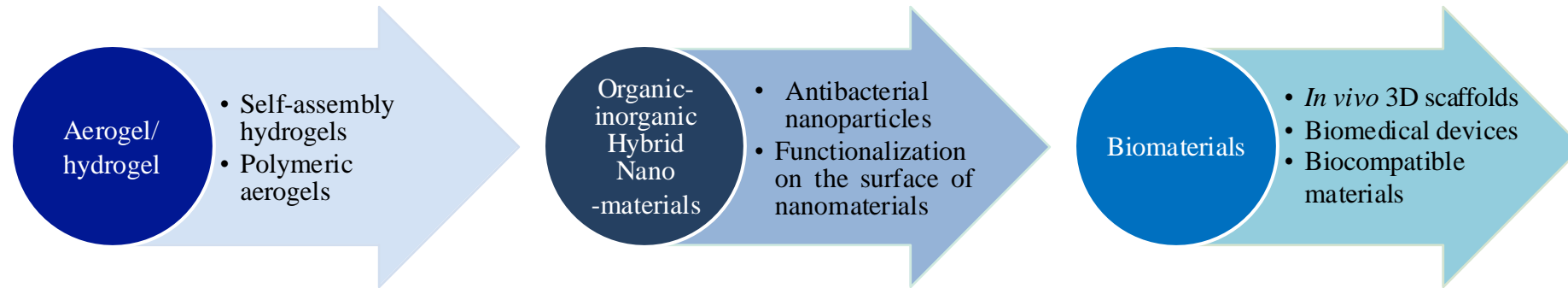


Figure 8. Agar dilution tests with carbon nanotube and titania nanoparticles P25@carbon nanotube solutions against GFP expressing *S. aureus* and *E. coli*



Future Research Plan





**Carnegie
Mellon
University**

Carnegie Mellon University is an ideal place to develop my capabilities for developing materials.

I would like to achieve my research goals and work together passionately at the Department of Material Science and Engineering.